Journal of Molecular Liquids 360 (2022) 119556

Contents lists available at ScienceDirect

Journal of Molecular Liquids

journal homepage: www.elsevier.com/locate/molliq

Gemini surfactant behavior of conventional surfactant dodecyltrimethylammonium bromide with anionic azo dye Sunset Yellow in aqueous solutions

Erol Akpinar [a,*], Nazli Uygur [a], Gokhan Topcu [a], Oleg D. Lavrentovich [b], Antônio Martins Figueiredo Neto [c]

[a] Bolu Abant Izzet Baysal University, Faculty of Arts and Sciences, Department of Chemistry, 14030 Golkoy, Bolu, Turkey
[b] Advanced Materials and Liquid Crystal Institute, Materials Science Graduate Program and Department of Physics, Kent State University, Kent, OH, USA
[c] Universidade de São Paulo, Instituto de Fisica, Rua do Matao, No. 1371, 05508-090 São Paulo, SP, Brazil

ARTICLE INFO

Article history:
Received 24 February 2022
Revised 7 May 2022
Accepted 3 June 2022
Available online 6 June 2022

Keywords:
Surfactant-dye interactions
Micellization parameters
Carpena's method
Aguiar's approach
Conventional surfactant
Gemini surfactant behavior
Electrical conductivity
UV–VIS spectroscopy

ABSTRACT

In this study, the interaction of an anionic azo dye Sunset Yellow with conventional cationic surfactant dodecyltrimethylammonium bromide (DTMABr) has been examined as a function of the dye concentration at 25 °C by electrical conductivity and UV–VIS spectroscopy measurements. Carpena's method, combined with Aguiar's approach, was applied to the analysis of the conductivity data for evaluating the micellization parameters such as critical micelle concentrations (cmc), degree of counterion bindings (β), and micellization Gibbs free energies ($\Delta_{mic}G$) from the specific conductivity-surfactant concentration curves. The UV–VIS absorption spectroscopy measurements were performed to obtain information on the dye concentration dependence of the stacking properties of Sunset Yellow in water. The results indicated that although DTMABr is a conventional surfactant with a single alkyl chain, it shows gemini surfactant behavior at relatively high dye concentrations as a result of the surfactant-dye interactions. To the best of our knowledge, this is the first study that shows both the gemini surfactant behavior of DTMABr in the presence of SSY and J-aggregations of SSY at high SSY concentrations in the presence of DTMABr. Furthermore, in the presence of DTMABr, the SSY molecules at low concentrations form H-aggregates; they show J-aggregation at high concentrations.

1. Introduction

Surfactant/dye interactions are important due to their applications in industry such as textile, photography, cosmetics, food, and pharmaceutical [1–5]. In the mixtures of surfactants/dyes, the nature and the strength of the interactions between surfactants and dyes play a key role in their applications [6]. In this respect, the suitable surfactant/dye systems are chosen and investigated by several methods such as conductivity, UV–VIS spectroscopy, surface tensiometry, potentiometry, and fluorescence [6–11]. In those mixtures, either conventional single-chain or gemini surfactants have been used. It was reported that the latter ones exhibit superior features with respect to the former one in some applications [11].

In the case of the oppositely charged surfactant/dye systems, some parameters affect the interactions between the surfactants and dyes [4,12–17]. Especially, the electrostatic/hydrophobic interactions between ionic surfactant and dye species [10,18], their chemical structures [19,20], and pH [6,21] are crucial for the formation of surfactant/dye aggregates. As it is expected, because the gemini surfactants have higher charge density on their head groups, they produce a stronger electrostatic interaction with oppositely charged dye molecules with respect to the conventional single-chain surfactants [4,11].

The surfactant-dye interactions are important not only in the diluted aqueous micellar solution of the surfactant/dye but also in lyotropic liquid crystals. In recent studies [22,23], it was observed that those interactions are responsible for the formation of different lyotropic structures, especially nematic ones. Those studies showed for the first time that the chaotropic/kosmotropic property of dye molecules plays a crucial role in micellar systems because this property determines the formation of the ion pairs/-complexes in the pre-micellar and binding the dye molecules to the micelle surfaces in the post-micellar regions.

Some azo dyes were used to investigate surfactant-dye interactions due to their important applications as organic colorants [5,11]. Most common ones are tartrazine [24,25], Sunset Yellow [6,11,17,26], amaranth [17,27], methyl orange [28,29], crystal vio-

* Corresponding author.
E-mail address: akpinar_e@ibu.edu.tr (E. Akpinar).

https://doi.org/10.1016/j.molliq.2022.119556
0167-7322/

let [29,30], congo red [31] etc. It was reported that azo dyes might form dye-surfactant complexes (D_xS_y) in aqueous submicellar solutions [28,31,32]. The formation of D_xS_y complexes may be well characterized by spectral shifts in the maximum absorption values by UV-VIS spectroscopy [33]. In these complexes, the association of dye with the surfactant molecule depends on the surfactant alkyl chain length. For instance, the surfactant alkyl chains consist of eight to twelve (thirteen to eighteen) —CH_2 groups, the complexes are formed by one (two) surfactant(s) per dye, i.e. DS (DS_2) complexes [32,34]. Furthermore, the extent of the interactions between ionic groups of dyes and surfactant ionic head groups is also important in the formation of dye-surfactant associations in the micellar solutions [23,31]. The characteristics of these interactions determine the organization of dye-surfactant complexes or ion pairs in the solutions as H-aggregations (face-to-face stacking or sandwich-type arrangement) or J-aggregations (head-to-tail stacking or slipped arrangement) [35–38]. Because the dyes have chromophore groups, the role of the interactions between dyes and surfactants on the formation of the aggregations can be seen in the loss of the absorbance of the chromophore groups [11,39,40] and the shift of λ_{max} [24]. While the former is evidence of the surfactant-dye interactions, the latter is related to the type of aggregations. A bathochromic (or "red") shift towards a longer wavelength with respect to the λ_{max} of the monomer dye in the absorbance spectra shows the presence of J-aggregates in surfactant-dye solutions [41]. Inversely, a hypsochromic or blue shift towards a shorter wavelength is evidence of the existence of H-aggregates in those solutions [41]. Thus, by analyzing the absorption spectra of dye solutions in the presence of the surfactants, how the surfactants encourage the dye aggregations is determined.

The surfactant-dye interactions were, in general, examined at very dilute dye concentrations in several studies. In the present study, we examined the surfactant-dye interactions at low and relatively high Sunset Yellow concentrations in DTMABr/water solutions. Some studies were reported for investigating the interaction of Sunset Yellow with cationic surfactants at constant low Sunset Yellow concentrations but, to the best of our knowledge, not at high concentrations. Electrical conductivity results showed that while Sunset Yellow exhibited similar interaction properties with a conventional single-chain DTMABr surfactant as reported in the literature, however, at high dye concentrations, DTMABr-Sunset Yellow solutions exhibit gemini-surfactant behavior. Furthermore, UV–VIS absorbance measurements indicate that at low (high) Sunset Yellow concentrations, the formation of H-aggregates (J-aggregates) is prevalent in the dye solutions as compared to J-aggregates (H-aggregates) in the absence of the surfactant.

2. Experimental

DTMABr (Sigma, ≥98%), dodecyltrimethylammonium chloride (DTMACl; Merck, ≥97), dodecyldimethylethylammonium bromide (DDMEABr; Sigma, ≥98%), tetradecyltrimethylammonium bromide (TTMABr; Sigma, 99%), hexadecyltrimethylammonium bromide (HTMABr; Merck, 97%) and sodium dodecylsulfate (SDS; Merck, ≥99%) were purchased. Potassium laurate (KL) was synthesized from the neutralization of lauric acid with potassium hydroxide, KOH, as described in Refs. [42,43]. It was confirmed that KL could be obtained with a purity of ≥99% by this synthesis procedure from the comparison of FT-IR spectra of KL and lauric acid (see Ref. [42] for the details). Sunset Yellow (SSY) was also commercially available from Sigma with a dye content of 90%. Because the purity of SSY is important for obtaining reliable and reproducible results, it was purified three times considering the procedure given in [44–46]. This procedure provides SSY with a purity of >99% [44,46]. Ultrapure water was provided by Millipore Direct-Q3 UV, which produces water having 18.2 MΩ·cm of resistivity at 25 °C for the preparation of isotropic micellar solutions.

Electrical conductivity measurements were performed in a Mettler Toledo S470 SevenExcellence conductivity meter at 25.0 °C to determine micellization parameters, critical micelle concentrations (cmc), degree of counterion bindings to the micelles (β), and micellization Gibbs free energies ($\Delta_{mic}G$). The dip-type conductivity cell was placed in a hand-made metallic (made from Al) sample holder in which water was circulated for providing stable temperature by the water circulating bath (Polyscience SD07R). The cell constant was read as 0.549231 cm^{-1} in the instrument and verified by using 0.1 M, 0.01 M, and 0.001 M KCl solutions [47]. The conductivities were measured as a function of the surfactant concentration by the successive addition of stock solutions of surfactants into the cell, including ultrapure water and SSY/water solutions, separately. The stock solutions were added by 10 μL micropipette (Eppendorf). To keep the water loss at the minimum level, the conductivity cell was closed well, except during the addition of the stock solution. For each surfactant/water and surfactant/SSY/water solution, the conductivities were measured at ~ 50 different total surfactant concentrations until reaching the concentration of the surfactant to about 2–2.5 times of the critical micelle concentrations. The measurements were repeated at least three times for each concentration by keeping, in general, the error limits <5–7%. The error limits in electrical conductivity results [48–52] were given in terms of coefficient of variation or relative standard deviation, which can be calculated from the ratio of standard deviation to the mean values [53], and presented in each table.

A Spectrum SP-UV 500VDB double beam spectrophotometer (Perkin Elmer Co.) was used for recording the UV-VIS absorption spectra of the Sunset Yellow/water solutions. The absorption spectra in the range of 300–700 nm with a 0.5 nm wavelength resolution were recorded using a pair of quartz cuvettes of 1.0 cm optical path. The quartz cuvettes, including water and the solutions, were kept on the reference side and the sample side, respectively. Both cuvettes were placed in the thermostated cell compartments at 25 °C. SSY/water solutions were prepared at different SSY concentrations in the range of 0.04–2.21 mmol/kg. Similar to the electrical conductivity measurements, the UV–VIS absorbance measurements were carried out at 25 °C. Each measurement was repeated at least three times, and the error limits in the measurements was <5–6%.

3. Results and discussions

3.1. Method to determine the critical micelle concentrations of the surfactants

The cmc of the surfactant molecules is determined with different methods [54,55]. The most common one is the measurement of the conductivity (κ) of the surfactant solutions as a function of the total surfactant concentration (C) [56]. Two different regions are observed in the κ-C graphs: the pre-micellar region below the cmc and the post-micellar region above the cmc. In both regions, the κ-C curves are linear with the slopes of S_1 and S_2, respectively, and the degree of counterion dissociation ($\alpha = S_2/S_1$) and then the degree of counterion binding ($\beta = 1 - \alpha$) are evaluated. When the transition occurs from the pre-micellar region to the post-micellar region, the change in the κ-C may be abrupt or gradual. In a conventional way (Williams's method [57]), the cmc can be determined from the intersection of two linear curves obtained in the pre- and post-micellar regions, separately. Although this way can

give the cmc values with small and acceptable uncertainties if the transition is abrupt, the gradual transition causes high uncertainties in the cmc values [58]. For the latter case, an alternative way was proposed by Carpena et al. [59] and applied to some surfactant solutions in the literature [52,60–62]. The first derivative of the κ-C curves gives a Boltzmann type sigmoid according to the following equation

$$\kappa = \frac{A_1 - A_2}{1 + e^{(C-C_0)/\Delta C}} + A_2 \quad (1)$$

where the parameters C_0, and A_1 and A_2 are the center of the width of the transition (ΔC), and slopes of the pre-micellar and post-micellar straight lines, respectively. Carpena's method proposes that if the first derivative of the κ-C curve of the experimental raw data is fitted to Eq. (1) to obtain the parameters, then, because the raw data need to behave as the integral of the sigmoid (Eq. (2)), the fitted conductivity data as a function of the surfactant concentration are determined from

$$\kappa = \kappa_0 + A_1 C + \Delta C(A_2 - A_1)\ln\left(\frac{1 + e^{(C-C_0)/\Delta C}}{1 + e^{-C_0/\Delta C}}\right) \quad (2)$$

The cmc value is precisely evaluated from the first derivative of the fitted data after the integration [58]. Furthermore, the degree of counterion dissociation is calculated from the ratio of A_2/A_1. For example, the experimental raw data and it's non-fitted first derivative for SDS/water are given in Fig. 1a, and their fitted curves are plotted in Fig. 1b, considering Carpena's method (Eq. (2)) for the comparison.

In 2003, Aguiar et al. considered an approach, which supports Carpena's method, to solve the problem of the precise determination of the cmcs of surfactants when the transition from pre-micellar region to the post-micellar one is gradual [63]. Their study was based on the pyrene 1:3 ratio method. In this method, the

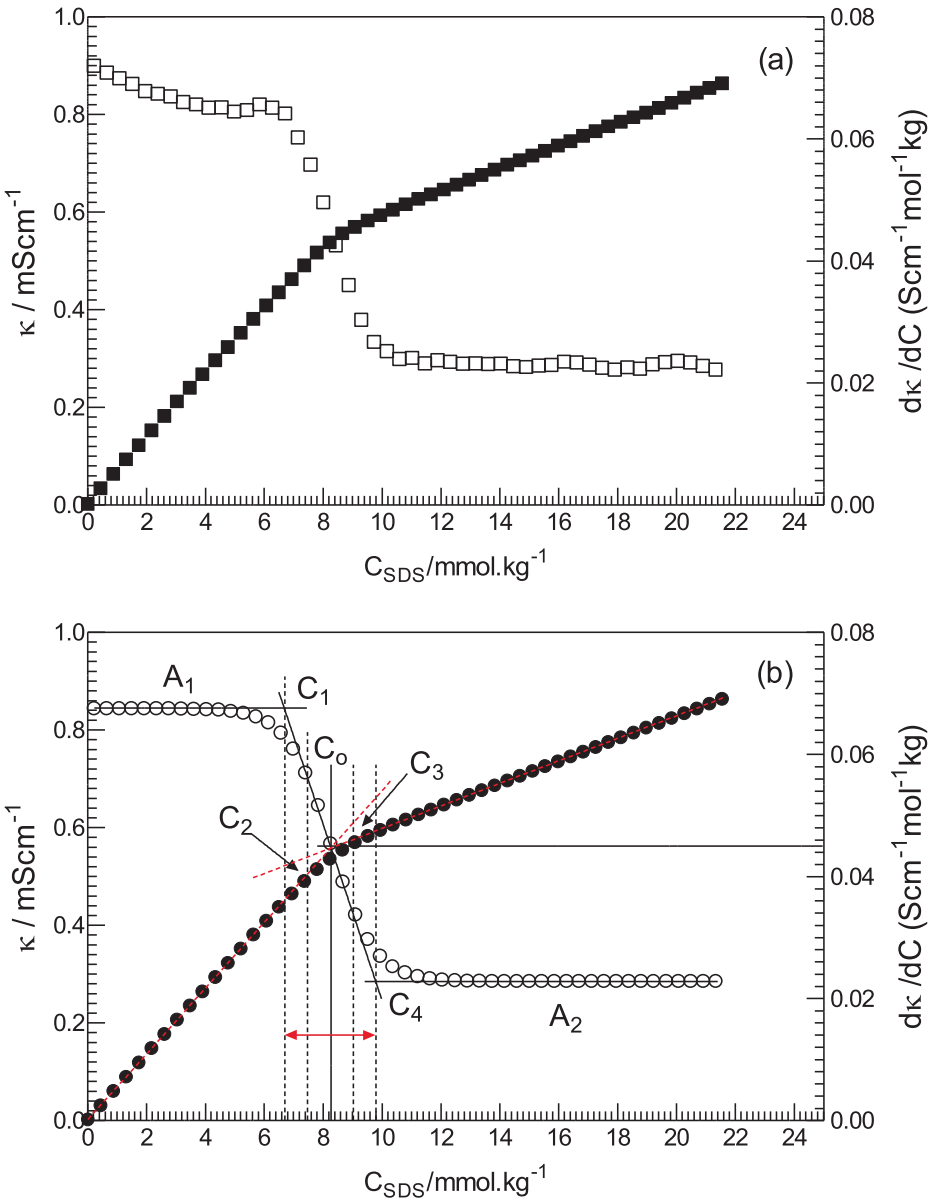

Fig. 1. (a) Conductivity versus total surfactant concentration (κ-C) curve of experimental raw data (■) and its non-fitted first derivative, dκ/dC, (□) for SDS/water solution at 25.0 °C. (b) Same curves were obtained from their fitted curves, (●) for κ-C and (○) for dκ/dC. The two-headed red arrow shows the total concentration distance (4ΔC), and it consists of four equal regions separated by vertical dashed lines, each of which corresponds to the concentration distance ΔC. (For interpretation of the references to color in this figure legend, the reader is referred to the web version of this article.)

pyrene 1:3 ratio decreases as a function of the surfactant concentration by giving a typical sigmoidal curve (Eq. (1)) similar to the one in the Fig. 1b. According to their treatments, the slope of the tangent line at the center of the sigmoid is

$$\left[\frac{d(I_1/I_3)}{dC}\right]_{C=C_0} = \frac{A_2 - A_1}{4\Delta C} \quad (3)$$

where C_0 still corresponds to the center of the sigmoid. After reorganization and simplifying some terms in the equations given in Ref. [63], the authors showed that there exists second cmc at $C_0 + 2\Delta C$. Our results are in good agreement with Aguiar's approach. In Fig. 1b, the tangent line intersects with A_1 and A_2 at the concentrations C_1 and C_4, respectively. The concentration distance between C_1 and C_4 corresponds to $4\Delta C$. Each part bordered by the dashed vertical lines before and after the center of the sigmoid (C_0) is equal to the ΔC. Until reaching the C_1, the conductivity of the solution increases linearly as the concentration of the solution increases with a constant slope. From C_1 to C_2 ($\approx C_1 + \Delta C$), the curve starts to be gradual, i.e., the transition from the monomer state of the surfactant to the micellar state begins. Further increase in the concentration from C_2 to C_0 ($\approx C_2 + \Delta C$) causes the curve to be more gradual. This can be seen from the deviation of the red-dashed straight line of the κ-C data. The opposite situation is observed from C_0 to C_3 ($\approx C_0 + \Delta C$) and from C_3 to C_4 ($\approx C_3 + \Delta C$). Especially, the transition at the concentration C_4 is important for discussing our results because it is equal to $C_0 + 2\Delta C$ as predicted by Aguiar et al. After the point C_4, the increase in the concentration of the surfactant leads to a linear increase in the conductivity with another constant slope, which is smaller than the one obtained before C_1. In other words, the micellization is completed, and the solution consists of stable micelles within the working concentration range. For other selected ionic surfactants (KL, DDMEABr, DTMACl, DTMABr, TTMABr and HDTMABr), the similar κ-C curves were obtained, Fig. 2. Their micellization parameters are given in Tables 1 and 2. The micellization Gibbs energies were calculated from the following equation [64]:

$$\Delta_{mic}G = (1 + \beta)RT\ln X_{cmc} \quad (4)$$

where R is the ideal gas constant (8.3145 J K^{-1} mol^{-1}), T is the absolute temperature (K), and X_{cmc} is the mole fraction of the surfactant at cmc.

Tables 1 and 2 show the micellization parameters (cmc, α, β and $\Delta_{mic}G$) for the surfactants at 25.0 °C, obtained in three different ways. The results are in good agreement with the literature values. Furthermore, Carpena's method, considering together with Aguiar's approach, seems us to be a more applicable way to DTMABr/SSY solutions because they exhibited the gradual transitions from the pre-micellar to the post-micellar region. In this way, we evaluated the micellization parameters of DTMABr/SSY solutions with lower uncertainties and investigated the DTMABr-SSY interactions at different SSY concentrations in the following part.

3.2. Behavior of micellar solutions of DTMABr with SSY

Sunset Yellow (disodium 6-hydroxy-5-[(4-sulfophenyl)azo]-2-naphthalenesulfonate) has an aromatic part and two ionic -SO_3^- moieties bound to the end regions of this part, Fig. 3. It is a 1:2 type

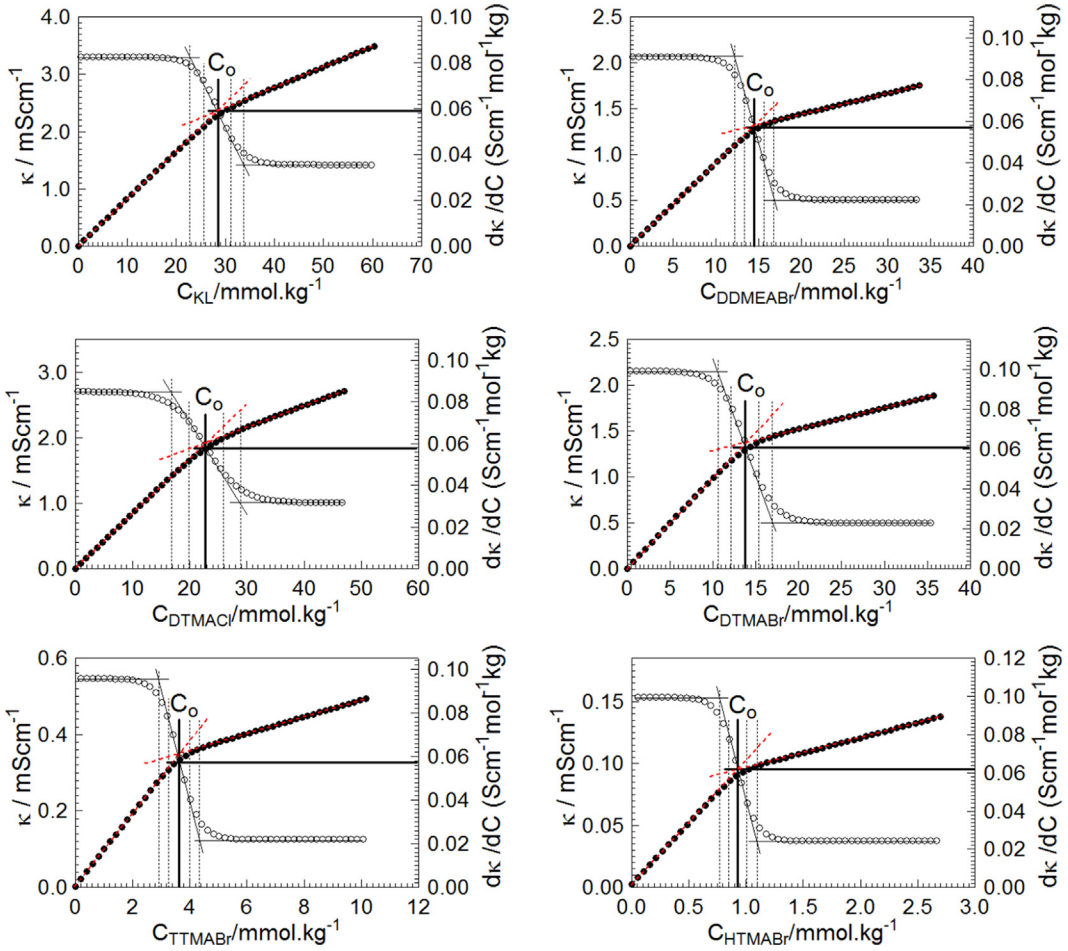

Fig. 2. Conductivity versus total surfactant concentration (●) and their first derivative (○) graphs for the surfactants, considering Carpena's method and Aguiar's approach.

Table 1
Critical micelle concentrations of the surfactant molecules at 25 °C, obtained from the conventional method, Boltzmann sigmoidal, and Carpena's method with Aguiar's approach. All concentrations are in mmol·kg^{-1}. The values in the parentheses are from the literature. The error limits are within 2% in cmc/C_o for all surfactant solutions.

Surfactant	Conventional method	Boltzmann sigmoidal (differentiation)						Carpena's method (integration)					
	CMC	ΔC	C_1	C_2	C_o	C_3	C_4	ΔC	C_1	C_2	C_o	C_3	C_4
SDS	8.30 (7.68–8.56[a–g,i])	0.73 (0.28 [h])	6.81	7.53 (7.62 [h])	8.26 (8.22 [h],8.29[i])	8.99	9.71	0.78	6.70	7.48	8.26 (8.28[i])	9.03	9.81
KL	28.39 (27.2[j])	2.65	23.04	25.69	28.34	30.98	33.63	2.71	22.91	25.63	28.34	31.05	33.76
DDMEABr	14.50 (14.0–15.2 [k–m])	1.05	12.37	13.43	14.48	15.53	16.59	1.15	12.19	13.33	14.48	15.63	16.77
DTMACl	22.86 (20.3–22.60[d,k,n–p])	2.98	16.84	19.82	22.81	25.79	28.77	3.01	16.78	19.79	22.81	25.82	28.83
DTMABr	13.84 (13.50–16.0[a,q–t])	1.95 (0.77 [h])	10.24	12.19	14.14 (13.60 [h])	16.09	18.04	2.09 (1.21[u])	9.91	12.00	14.08 (15.6[u])	16.18	18.27
TTMABr	3.67 (3.60–3.78[i,s,t,v,w])	0.32 (0.21 [h])	2.99	3.31	3.63 (3.73[i])	3.95	4.27	0.35 (0.138[u])	2.93	3.28	3.63 (3.75[i])	3.98	4.33
HTMABr	0.931 (0.92–1.00[a,i,w,y])	0.064 (0.057 [h])	0.799	0.863	0.928 (0.96[i])	0.992	1.06	0.079 (0.121[u])	0.770	0.848	0.927 (0.97[i])	1.01	1.08

[a][65], [b] [66], [c] [67], [d] [68], [e] [29], [f] [69], [g] [30], [h] [63], [i] [59], [j] [70], [k] [71], [l] [72], [m] [73], [n] [74], [o] [75], [p] [76], [q] [77], [r] [11], [s] [78], [t] [79], [u] [80], [v] [81], [w] [82], [y] [83].

electrolyte and it ionizes in water to give one SSY^{2-} anion and two Na^+ cations per unit formula. It was proved that the SSY molecule is in hydrazone form rather than azo form in an aqueous medium [46]. The hydrogen bond in the hydrazone form provides it to exhibit a stable planar structure [41].

Before discussing the results of DTMABr-SSY solutions, it would be useful to mention some studies given in the literature. Shahir et al. [24] investigated the properties of surfactant/dye solutions composed of anionic azo dye tartrazine, like Sunset Yellow, and single-chain conventional surfactant and gemini surfactants by electrical conductivity. The conventional surfactant was TTMABr, and gemini surfactants were N,N'-ditetradecyl-N,N,N',N'-tetramethyl-N,N'-butanediyl-diammonium dibromide (14,4,14) and N,N'-didodecyl-N,N,N',N'-tetramethyl-N,N'-butanediyl-diammonium dibromide (12,4,12). If tartrazine-added solution is compared with tartrazine-free TTMABr/water solution, the cmc of TTMABr decreased slightly from 3.67 mM to 3.60 mM and in both cases the conductivity of the solutions increased linearly from starting point (C_{TTMABr} = 0.00 mM) to the cmc of TTMABr. However, in the case of the presence of the gemini surfactants, the conductivity of the solutions increased slightly at very low surfactant concentrations, then increased more sharply and linearly until reaching the cmcs of the gemini surfactants. Furthermore, the transition from monomer state to micellar state turned into more gradual by giving two more break points on the conductivity-surfactant concentration curve. In another study, Fazeli et al. [11] examined the surfactant-dye interactions in the DTMAB/SSY solutions at a fixed SSY concentration (0.04 mM) via surface tension, UV–VIS spectroscopy and zeta potential measurements, but not via electrical conductivity. They reported the decrease in the cmc of DTMABr from 14.85 mM to 8.46 mM by the addition of SSY to the solution. However, Nazar and Murteza [6] stated that the presence of SSY (0.044 mM) changed the cmc of HTMABr from 0.9 mM to 1.18 mM, although the concentration of SSY was greater than in Fazeli et al. study [11]. In addition, it was shown that the addition of another azo dye, methyl orange (1.01 mM), slightly increased the cmcs of DTMABr, SDS and TX-114 surfactants from 14.43 mM, 8.00 mM and 0.24 mM to 14.48 mM, 8.11 mM and 0.25 mM, respectively [29]. It is seen that the addition of methyl orange slightly changed the cmcs of the surfactants. A similar situation was also reported for cetyltrimethylammonium bromide/reactive red 223 mixtures [87]. Summarily, in general, for low dye concentrations, the cmcs of surfactants slightly change or remain unchanged in the presence of dye molecules.

Fig. 4 shows the total DTMABr concentration-dependence of specific conductivity of the DTMABr/SSY/water solutions at different SSY concentrations. As it can be seen, except 0.04 mmol/kg SSY concentration, the behavior of the curves is similar to that of gemini surfactant/tartrazine solutions [24] at low DTMABr concentrations, and as the concentration of SSY increases this behavior is more dominant (Fig. 4). The region, bordered by red-dashed line rectangular in Fig. 4, was investigated more precisely (Fig. 5). As

Table 2
Degrees of counterion dissociation and binding, and micellization Gibbs free energy of the surfactant molecules at 25 °C, evaluated from the cmc values given in Table 1. The values in the parentheses are from the literature. The error limits are within 3%, 5% and 2% in α, β and $\Delta_{mic}G°$ for all surfactant solutions, respectively.

Surfactant	Conventional method			Boltzmann sigmoidal (differentiation)			Carpena's method (integration)		
	α	β	$\Delta_{mic}G°$/kJ·mol^{-1}	α	β	$\Delta_{mic}G°$/kJ·mol^{-1}	α	β	$\Delta_{mic}G°$/kJ·mol^{-1}
SDS	0.344 (0.369[a])	0.656 (0.62[b])	−36.13 (−35.46[b])	0.351 (0.369[a])	0.649	−36.02	0.334 (0.368[a])	0.666	−36.37
KL	0.435	0.565	−29.38	0.424	0.576	−29.60	0.423	0.577	−29.62
DDMEABr	0.254 (0.261[c])	0.746	−35.68 (−35.60[c])	0.249	0.751	−35.80	0.247	0.753	−35.83
DTMACl	0.390 (0.389[c])	0.610	−31.15 (−30.56[d], −31.43[c])	0.366	0.634	−31.56	0.366	0.634	−31.57
DTMABr	0.242 (0.244–0.281[a,e–h])	0.758 (0.75–0.756[e,h])	−36.19 (−34.81–−36.0[e,g,h])	0.232 (0.251[a])	0.768	−36.39	0.229 (0.248[a])	0.771 (0.75[i])	−36.33 (−35.48[i])
TTMABr	0.235 (0.227, 0.23[a,j])	0.765 (0.77[j])	−42.10 (−42.10, −42.30[j,k])	0.229 (0.231[a])	0.771	−42.27	0.228 (0.230[a])	0.772 (0.76[i])	−42.3 (−41.83[i])
HTMABr	0.255 (0.243[a])	0.745 (0.77[b])	−47.50 (−46.45–−48.30[b,k,l])	0.251 (0.250[a])	0.749	−47.66	0.248 (0.241[a])	0.752 (0.76[i])	−47.76 (−47.86[i], 48.1 [l])

[a][59], [b] [66], [c] [71], [d] [76], [e] [84], [f] [73], [g] [85], [h] [85], [i] [80], [j] [86], [k] [81], [l] [60].

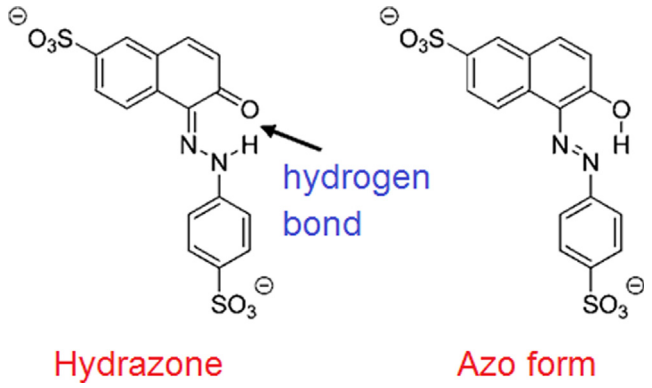

Fig. 3. The tautomeric forms of the Sunset yellow molecule [41]. (For interpretation of the references to color in this figure legend, the reader is referred to the web version of this article.)

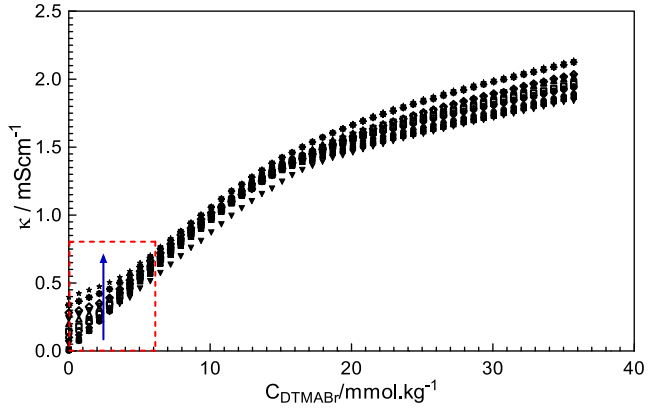

Fig. 4. DTMABr concentration dependence of specific conductivity at different SSY concentrations (0.04–2.21 mmol/kg). Blue arrow shows the direction along which the SSY concentration increases in the solutions. Within the region bordered by the red-dashed line rectangular, the gemini surfactant behavior in the presence of dye was observed. (For interpretation of the references to color in this figure legend, the reader is referred to the web version of this article.)

the concentration of the DTMABr increases there are two more breakpoints on the curve, which were labeled as concentrations C_p and C_C, respectively, in this study. The appearance of these points was attributed to the formation of J-aggregation/precipitation/redissolution process as reported for TTMABr/tartrazine solutions [24]. It means that DTMABr causes the formation of H-aggregation of SSY molecules at 0.04 mmol/kg SSY concentration, as reported for this concentration of SSY in the literature [11], and it encourages the J-aggregation of SSY at the SSY concentrations ≥0.168 mmol/kg. Fig. 6a shows the SSY concentration dependence of the concentration C_C, and it can be seen that as the concentration of the SSY increases the formation of the J-aggregates is more favored.

Some dye molecules may spontaneously aggregate, depending on dye concentrations, to form stacks as dimers, trimers, tetramers,... in aqueous solutions [24,31,88,89]. The formation of dye stacks affects the polar environment around chromophore groups and this situation causes the change in the UV-VIS absorption spectra of dye-surfactant solutions. To clarify whether dye stacking affects gemini surfactant behavior (Figs. 4 and 5) of DTMABr-SSY solutions, UV-VIS absorption spectra (Figs. 6 and 7) and conductivity (Fig. 8a) of SSY solutions as a function of SSY concentration in the absence of DTMABr were studied. In other words, before discussing the interactions between DTMABr and SSY, it would be better if we examine the interactions between SSY molecules in the absence of DTMABr in the solutions to understand whether the SSY-stacking plays a role on gemini surfactant behavior of DTMABr in the presence of SSY. Figs. 6 and 7 show the spectral changes observed at low and relatively higher SSY concentrations in the absence of DTMABr. Fig. 6 exhibits UV–VIS spectra of dye solutions at dilute SSY concentrations. Until ~0.10 mmol/kg SSY-concentration, the dye solutions obey Beer-Lambert's law, exhibiting linear change with SSY concentrations, however, deviations were observed >0.10 mmol/kg (Fig. 8b). These deviations arise from interactions between the absorbing species (i.e. chromophore groups of SSY) and to alterations of the refractive index of the medium. It is known that if dye molecules are present in the solution as monomers and no interaction occurs between them, the solution

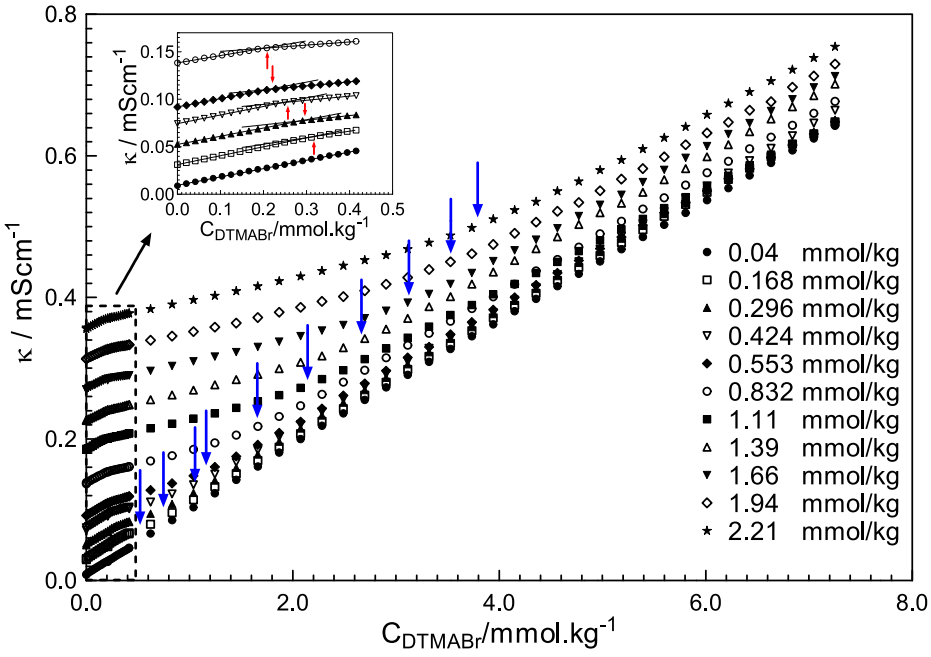

Fig. 5. Specific conductivity versus DTMABr concentrations at different SSY concentrations (4.00–2.21 mmol/kg). The blue arrows correspond C_C values. (Inset) The red arrows show C_p concentrations between 0.04 and 0.832 mmol/kg SSY. The SSY concentrations > 0.832 mmol/kg give similar specific conductivity curves and C_p values with 0.832 mmol/kg SSY. (For interpretation of the references to color in this figure legend, the reader is referred to the web version of this article.)

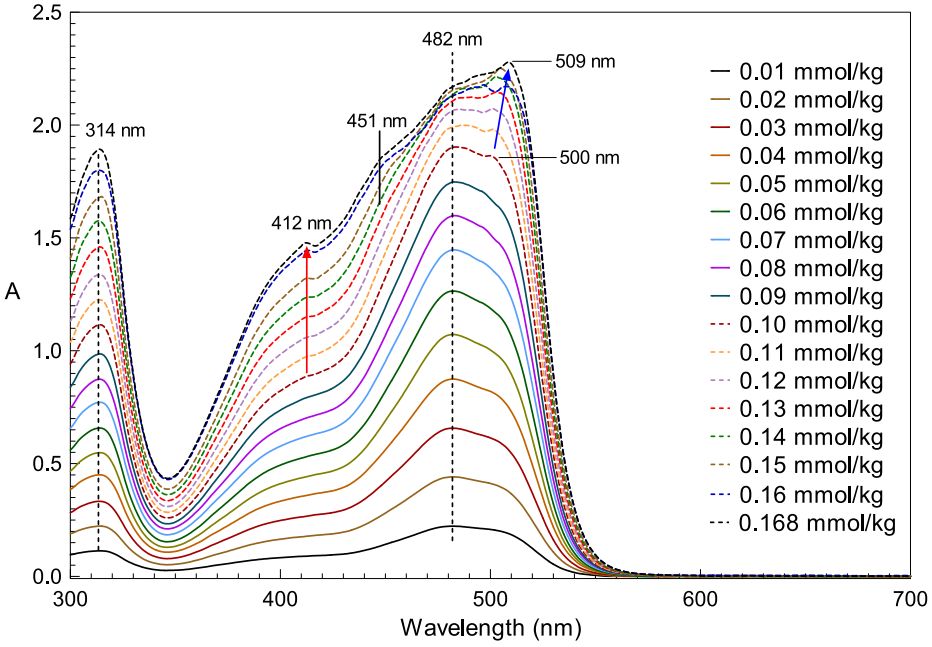

Fig. 6. UV-VIS absorption spectra of SSY/water solutions varying the SSY concentrations between 0.01 and 0.168 mmol/kg in the absence of surfactant at 25 °C.

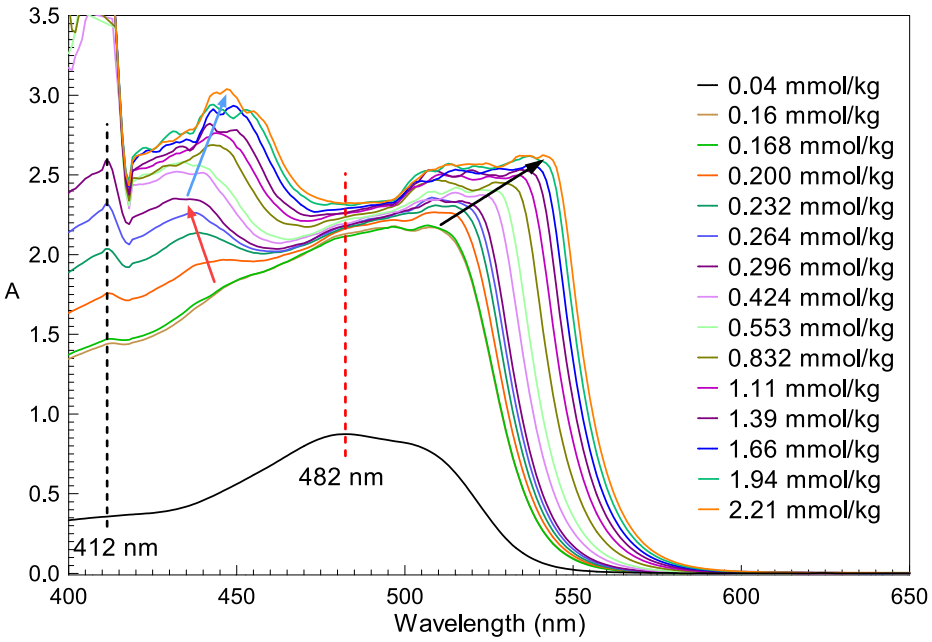

Fig. 7. UV-VIS absorption spectra of SSY/water solutions varying the SSY concentrations between 0.200 and 2.21 mmol/kg in the absence of surfactant at 25 °C. The spectra for 0.04, 0.16 and 0.168 mmol/kg SSY concentrations are given in this figure for comparison.

obeys the law, i.e. dyes molecules do not self-aggregate due to the repulsive forces between the similarly charged parts of the dye molecules. Conversely, deviations from the law are observed if dye molecules interact with one another, which results in dye stacking. Thus, the deviations observed for SSY-concentrations >0.10 mmol/kg (in the absence of DTMABr, Fig. 8b) are attributed to the SSY-stacking as a result of π-π attractive interactions between dye molecules, which dominates the electrostatic repulsions between negatively charged -SO_3^- groups of SSY molecules.

Now, let's investigate Figs. 6 and 7 in detail to find information on the aggregation behavior of SSY within the working concentration range, i.e. existing as a monomer or higher-order aggregate in the absence of DTMABr. It is known that the monomer SSY molecule has two absorption bands: a major one, which has a maximum around 480–482 nm, and a second one at ~314 nm [11,90,91]. While the major absorption band is related to the color of SSY due to the n-π* transition absorption of the chromophore groups of SSY molecule [91], the second one arises from the π-π* transition absorption related to the aromatic rings of SSY molecules [92,93]. For 0.04 mmol/kg, SSY exhibits characteristic UV–VIS absorption spectra given in the literature (Fig. 9) [11]. Until the SSY-concentration reaches the concentration, at which the devia-

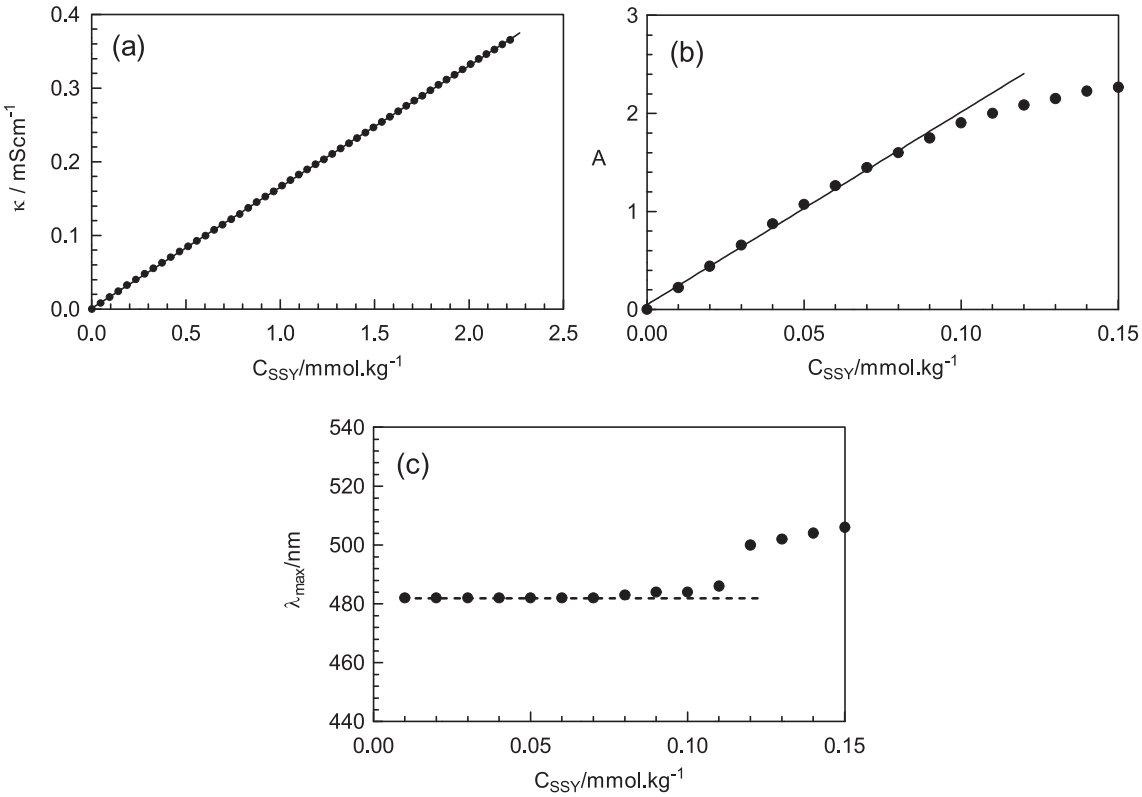

Fig. 8. SSY concentration dependences of (a) specific conductivity, (b) absorbance, and (c) wavelength of maximum absorption in the concentration range of 0.00–2.21 mmol/kg at 25 °C in the absence of DTMABr.

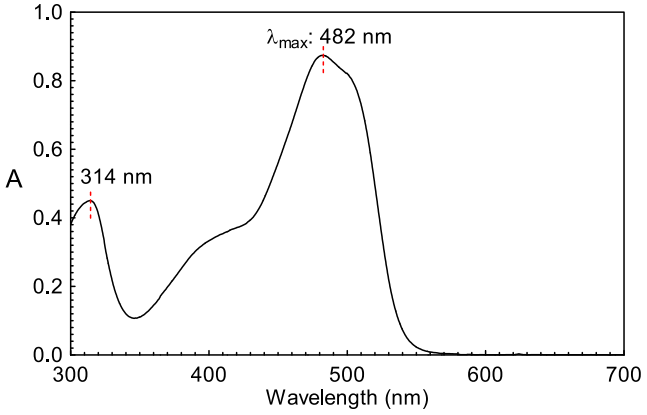

Fig. 9. UV-VIS absorption spectrum of 0.04 mmol/kg SSY solution at 25 °C in the absence of surfactant.

tion from the Beer-Lambert's law starts (~0.10 mmol/kg), similar spectra for C_{SSY} < 0.10 mmol/kg were recorded (Fig. 6). However, at SSY concentrations > 0.10 mmol/kg, three new bands can be seen: at 412 nm, 451 nm and 500 nm. There is no maximum wavelength shift for the band at 412 nm but its intensity increases as the concentration of SSY increases, especially C_{SSY} > 0.296 mmol/kg. The band at 451 nm shifts to 435 nm (blue shift) then to 445 nm (red shift) and the intensity of maximum absorption slightly increases within the chosen concentration range of SSY. The absorption band at 500 nm continuously shifts to a higher wavelength (red shift) as a relatively broad peak. The main change in the UV–VIS spectra of the monomer SSY is observed around the major band. At low concentrations (C_{SSY} < 0.10 mmol/kg) the maximum absorption of the major band is seen at 482 nm with no additional bands and the maximum absorption at 482 nm starts to disappear as the concentration of the SSY increases for C_{SSY} > 0.10 mmol/kg (Fig. 6). Especially, for C_{SSY} > 0.200 mmol/kg, no maximum absorption band at 482 nm was observed in the UV–VIS spectra. Because this band is related to the existence of SSY monomers in the solutions, at high SSY concentrations, this situation may be attributed to the absence of SSY as monomers in the solutions. To make a comprehensive interpretation of UV-VIS spectra of SSY solutions, we must consider two maximum absorption bands at 435 nm and 500 nm in the case of the disappearance of the band at 482 nm. At low SSY concentration, first, the intensity of the band at 482 nm decreases, and that at 500 nm increases with the red shift. This situation continues until the band at 482 nm is disappeared. At the same time, the band at 435 nm shifts towards 445 nm. Note that the maximum absorption is observed in wavelengths >500 nm (red shift). For further increase in the SSY concentration, now the band at 435 nm turned to be wavelength at which maximum absorption is observed with red shift. Consequently, in both cases, the shifts from 435 nm to 445 nm and from 500 nm to ~550 nm mean that the formation of J-aggregation of SSY is more probable for C_{SSY} > 0.296 mmol/kg. In other words, at low (high) surfactant concentrations, the SSY molecules form H-aggregates as shown in the literature (J-aggregates). This is in good agreement with the conductivity results. Furthermore, the beginning of the formation of J-aggregates after C_{SSY} > 0.100 mmol/kg is supported with the red shift in the λ_{max} values as a function of the increase in the SSY-concentration (Fig. 8c).

Fig. 7 also include information about the aggregation order of the SSY molecules in the absence of DTMABr. In a recent study, Fernandez-Perez and Marban analyzed the UV–VIS absorption spectra of methylene blue (MB) azo dye aggregation in water [94]. They studied the UV–VIS spectra of MB solutions for its large concentration range, 1.1×10^{-6}–3.4×10^{-3} M, where the last con-

Table 3
SSY concentration dependence of micellization parameters of DTMABr at 25.0 °C obtained from electrical conductivity measurements, considering the Carpena's method. The error limits are within 7%, 7%, 3% and 2% in cmc (C_o), α, β and $\Delta_{mic}G°$ for all SSY concentrations, respectively.

SSY/mmol·kg^{-1}	C_p/mmol·kg^{-1}	C_C/mmol·kg^{-1}	ΔC/mmol·kg^{-1}	C_1/mmol·kg^{-1}	C_o/mmol·kg^{-1}	C_4/mmol·kg^{-1}	α	β	$\Delta_{mic}G$/kj·mol^{-1}
0.000	–	–	2.09	9.91	14.08	18.27	0.229	0.771	−36.33
0.040	–	–	1.93	9.83	14.15	18.47	0.231	0.769	−36.26
0.168	0.31	0.50	2.07	9.72	14.23	18.69	0.233	0.767	−36.20
0.296	0.29	0.75	2.34	9.64	14.38	19.02	0.237	0.763	−36.07
0.424	0.25	1.05	2.52	9.50	14.45	19.46	0.238	0.762	−36.03
0.553	0.22	1.17	2.57	9.41	14.56	19.70	0.242	0.758	−35.91
0.832	0.20	1.65	3.09	9.19	14.77	20.31	0.248	0.752	−35.73
1.11	0.18	2.12	3.36	8.88	15.09	21.44	0.252	0.748	−35.56
1.39	0.20	2.66	3.45	8.60	15.36	22.32	0.257	0.743	−35.38
1.66	0.18	3.13	3.64	8.31	15.57	22.85	0.265	0.735	−35.16
1.94	0.19	3.53	3.92	8.15	15.74	23.30	0.270	0.730	−35.01
2.21	0.17	3.79	4.21	7.97	16.01	24.23	0.277	0.723	−34.79

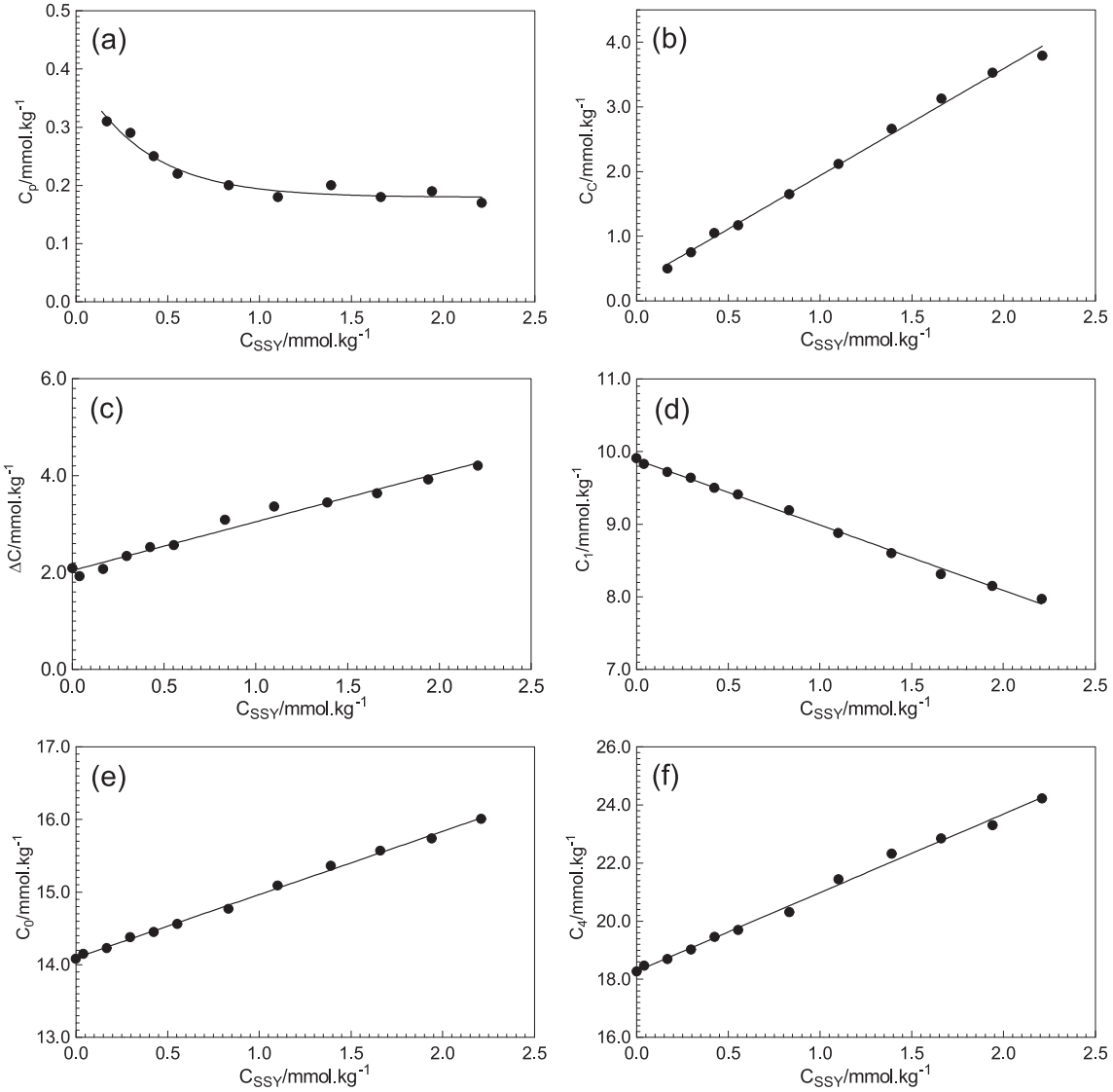

Fig. 10. SSY concentration dependences of (a) C_p and (b) C_C from Williams's method, and (c) ΔC, (d) C_1, (e) C_0 and (f) C_4 considering Carpena's method and Aguiar's approach.

centration of MB is about 1.5 times greater than that of SSY used in the present study. The monomer MB gives a major band around 660 nm with a shoulder at 612 nm. As the concentration increases the absorption intensity of the band at 660 nm decreases while the maximum absorption is observed at 607 nm by shifting the wavelength of the band at 612 nm, i.e., there exist two bands with a maximum at 607 nm, which corresponds to the formation of dimer as a result of MB stackings. Further increase in the MB-concentration causes the disappearance of the band at 660 nm and shifting the maximum wavelength to 600 nm (blue shift) with relatively higher absorption intensity. The latter situation was attributed to the formation of tetramers of MB dyes. Almost similar

results were obtained in our study (Fig. 7). Thus, we can say that, at the relatively low SSY concentrations >0.10 mmol/kg, the dimer formation is observed and, approaching to 2.21 × 10^{-3} mol/kg SSY-concentration, the higher-order aggregate formation of SSY (tetramer or higher-order, considering the Ref. [94]) is more probable. Consequently, it can be concluded that while H-aggregates as dimers are formed at low SSY-concentrations, J-aggregate formations are favored as a higher-order at high SSY-concentrations. However, the formation of dye stacking as H/J-aggregates does not affect the conductivity of aqueous dye solutions with respect to that of dye molecules in a monomer state. The conductivity of SSY solutions exactly shows linear change with the concentration of SSY (Fig. 8a). Thus, the gemini surfactant behavior of DTMABr/SSY obtained in the conductivity curves of DTMABr/SSY solutions (Figs. 4 and 5) can not be attributed to the SSY stackings. Instead, it is clear that this behavior should be a result of surfactant/dye interactions.

After clarifying that SSY-stacking has no effect on the gemini surfactant behavior of DTMABr in the presence of SSY, we may proceed with discussing the analysis of conductivity results of aqueous DTMABr/SSY solutions as a function of SSY concentration in the solutions. Because the transition from monomer state to the micellar state gets more gradual around the cmc of DTMABr (Fig. 4), Carpena' method, considering Aguiar's approach, was applied to DTMABr/SSY solutions to evaluate their micellization parameters. For the calculations, C_C, C_1, C_0 and C_4 are important but C_2 and C_3 not: the linear curves between C_C and C_1 in the pre-micellar region and above C_4 (post-micellar region) were used to find α and β values, and then $\Delta_{mic}G$. All values depending on SSY concentrations are given in Table 3. Furthermore, those values were plotted against SSY concentrations in Figs. 10 and 11.

By increasing the C_{SSY}, the C_1 values decrease (Fig. 10d) and C_4 ones increase (Fig. 10f), which indicates the increase in the concentration range ΔC (Fig. 10c). Furthermore, the cmc of DTMABr is unfavored (Fig. 10e) as supported by the change in β and $\Delta_{mic}G$. It is known that if the micellization is less favored the number of counterions bound to the surfactant head groups on the micelle surfaces decreases, i.e. smaller β (Fig. 11b) or greater α (Fig. 11a). Besides, the micellization Gibbs energy takes fewer negative values (Fig. 11c).

The change in the values of α as a function of Sunset Yellow concentration includes some useful information (Fig. 11a and b, respectively) on the location of Sunset Yellow molecules around the micelle surfaces. Two important factors affect the change in the value of α: (a) electrostatic attractive interactions between the counterions and the head groups of the surfactants on the micelle surfaces and (b) the change in the thermal energy with temperature. Those factors have opposite effects on the value of α. The first factor causes the decrease in the value of α, i.e. the increase in the value of β, because the attractions between the counterions and the surfactant head groups promote either the binding of a large number of counterions or strong binding of the counterions to the surfactant head groups at the micelle surfaces. However, the second one enhances the increase in the thermal energy with temperature and, consequently, dissociation of the counterions from the surfactant head groups, i.e., an increase in α. Although the α values increases, as observed for the second factor, with the concentration of Sunset Yellow, this cannot be related to the increase in the thermal dissociation of the counterions from the head groups because the temperature is constant in our experimental study. Thus, the increase in the values of α is attributed to the presence of Sunset Yellow close to the micelle surfaces, which causes steric hindrance for the binding of the counterions of DTMABr (Br^- ions) to the micelle surfaces, as reported for another anionic azo dye, tartrazine, and tetradecyltrimethylammonium bromide solutions [25]. So, it is clear that the gemini surfactant behavior of DTMABr at relatively high SSY concentrations is a result of the stronger interactions between the cationic head groups of DTMABr, $-N^+(CH_3)_3$, and the two anionic parts of SSY, $-SO_3^-$, than $-N^+(CH_3)_3$ and Br^-. This situation arises from the similar chaotropic characters of both $-N^+(CH_3)_3$ and $-SO_3^-$ as recently shown in the literature, i.e. the higher the similar character means the stronger interactions between two ionic species [22,23].

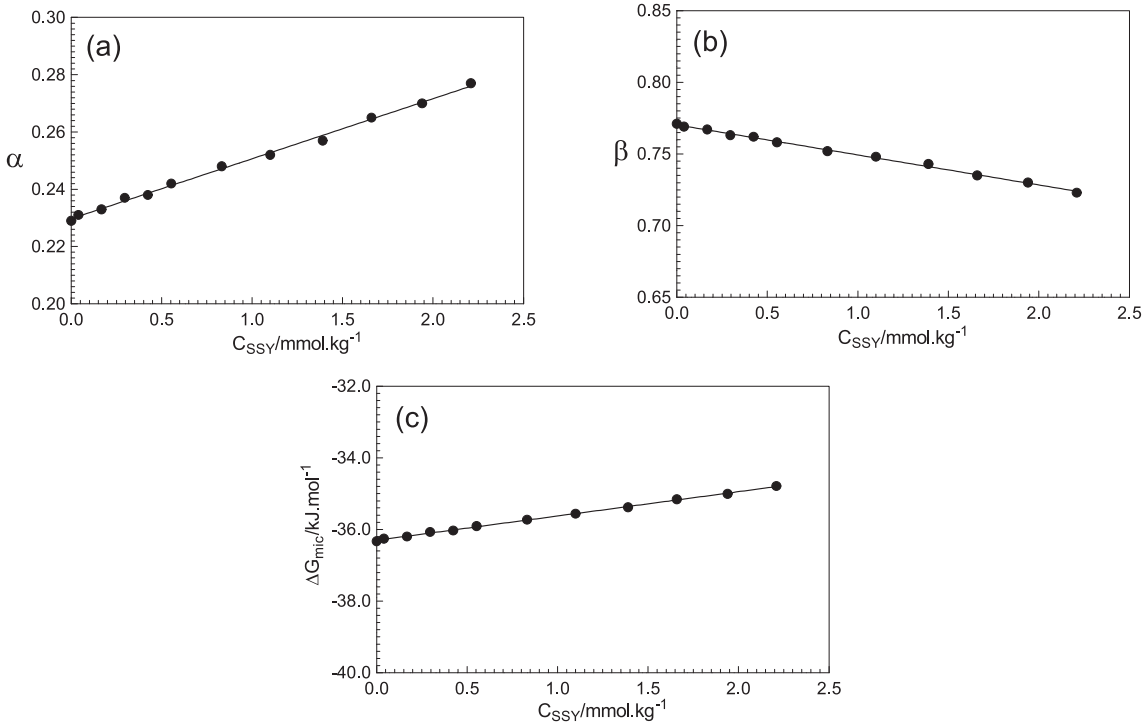

Fig. 11. Changes in α, β and $\Delta_{mic}G$ as a function of SSY concentration in the solutions.

4. Conclusions

In the present study, we investigated the surfactant-dye interactions between cationic surfactant DTMABr and anionic azo dye Sunset Yellow. Differently from the existing studies on the aqueous DTMABr-SSY solutions in the literature, the properties of those solutions were studied at a relatively larger SSY concentration range. It was surprisingly observed that although DTMABr is a conventional single-chain surfactant, it exhibited gemini surfactant behavior at high SSY concentrations, as reported for tartrazine-gemini surfactant system, as a result of the surfactant-dye interactions. For low SSY concentrations, that behavior was not observed, which is in good agreement with the literature. Furthermore, in the presence of DTMABr, the SSY molecules at low concentrations form H-aggregates, they show J-aggregation at high concentrations. To the best of our knowledge, this is the first study that shows both the gemini surfactant behavior of DTMABr in the presence of SSY and J-aggregations of SSY at high SSY concentrations in the presence of DTMABr. Considering the application of SSY in cosmetic, food, etc., this study includes some useful merits.

Author contribution statement

Erol Akpinar (EA), Antonio M. F. Neto (AMFN) and Oleg D. Lavrentovich (ODL) designed the experimental parts of the studies, then analyzed and discussed the results. Nazli Uygur (NU) and Gokhan Topcu (GT) performed the experimental work.

Declaration of Competing Interest

The authors declare that they have no known competing financial interests or personal relationships that could have appeared to influence the work reported in this paper.

Acknowledgements

EA thanks the Scientific and Technological Research Council of Turkey (TÜBİTAK, grant number: 217Z079); Bolu Abant Izzet Baysal University Directorate of Research Projects Commission (BAP, grant number: 2021.03.03.1505) for supporting this work. ODL research was supported by the U.S. National Science Foundation (grant no: DMS-2106675). AMFN acknowledges financial support from INCT/CNPq (Conselho Nacional de Desenvolvimento Científico e Tecnológico; Grant number: 465259/2014-6), INCT/FAPESP (Fundação de Amparo à Pesquisa do Estado de São Paulo; Grant Number: 14/50983-3), INCT/CAPES (Coordenação de Aperfeiçoamento de Pessoal de Nível Superior; Grant number: 88887.136373/2017-00), FAPESP (Thematic Project; Grant 2016/24531-3), and INCT-FCx (Instituto Nacional de Ciência e Tecnologia de Fluidos Complexos).

References

[1] E. Nürnberg, W. Pohler, Zur Kenntnis von 3-Komponenten-Mikroemulsionsgelen. Surfactants, Micelles, Microemulsions and Liquid Crystals., in: Weiss (Ed.), Progress in Colloid & Polymer Science, 69, Steinkopff, Darmstadt, 1984, pp. 48–55.
[2] J. Yang, Interaction of surfactants and aminoindophenol dye, J. Colloid Interface Sci. 274 (1) (2004) 237–243, https://doi.org/10.1016/j.jcis.2004.03.028.
[3] S.M. Ghoreishi, M.S. Nooshabadi, Electromotive force studies about some dyes–cationic surfactants interactions in aqueous solutions, Dyes Pigm. 65 (2) (2005) 117–123, https://doi.org/10.1016/j.dyepig.2004.07.004.
[4] A.R. Tehrani Bagha, H. Bahrami, B. Movassagh, M. Arami, F.M. Menger, Interactions of gemini cationic surfactants with anionic azo dyes and their inhibited effects on dyeability of cotton fabric, Dyes Pigm. 72 (3) (2007) 331–338, https://doi.org/10.1016/j.dyepig.2005.09.011.
[5] M.R. Almeida, R. Stephani, H.F. Dos Santos, L.F.C.d. Oliveira, Spectroscopic and theoretical study of the "azo"-dye E124 in condensate phase: evidence of a dominant hydrazo form, J. Phys. Chem. A 114 (1) (2010) 526–534, https://doi.org/10.1021/jp907473d.
[6] M.F. Nazar, S. Murtaza, Physicochemical investigation and spectral properties of Sunset Yellow dye in cetyltrimethylammonium bromide micellar solution under different pH conditions, Color. Technol. 130 (2014) 191–199, https://doi.org/10.1111/cote.12085.
[7] B. Simončič, J. Špan, A study of dye–surfactant interactions. Part 3. Thermodynamics of the association of C.I. Acid Orange 7 and cetylpyridinium chloride in aqueous solutions, Dyes Pigm. 46 (1) (2000) 1–8, https://doi.org/10.1016/S0143-7208(00)00035-8.
[8] M.S. Chauhan, N. Kumari, S. Pathania, K. Sharma, G. Kumar, A conductometric study of interactions between gelatin and sodium dodecyl sulfate (SDS) in aqueous-rich mixtures of dimethylsulfoxide, Colloids Surf. A 293 (1–3) (2007) 157–161, https://doi.org/10.1016/j.colsurfa.2006.07.020.
[9] R. Hosseinzadeh, R. Maleki, A.A. Matin, Y. Nikkhahi, Spectrophotometric study of anionic azo-dye light yellow (X6G) interaction with surfactants and its micellar solubilization in cationic surfactant micelles, Spectrochim. Acta A 69 (4) (2008) 1183–1187, https://doi.org/10.1016/j.saa.2007.06.022.
[10] N. Hashemi, G. Sun, Intermolecular interactions between surfactants and cationic dyes and effect on antimicrobial properties, Ind. Eng. Chem. Res. 49 (18) (2010) 8347–8352, https://doi.org/10.1021/ie101001d.
[11] S. Fazeli, B. Sohrabi, A.R. Tehrani-Bagha, The study of sunset yellow anionic dye interaction with gemini and conventional surfactants in aqueous solution, Dyes Pigm. 95 (3) (2012) 768–775, https://doi.org/10.1016/j.dyepig.2012.03.022.
[12] Ç. Kartal, H. Akbaş, Study on the interaction of anionic dye–nonionic surfactants in a mixture of anionic and nonionic surfactants by absorption spectroscopy, Dyes Pigm. 65 (3) (2005) 191–195, https://doi.org/10.1016/j.dyepig.2004.07.003.
[13] M. Nasiruddin Khan, A. Sarwar, Study of dye–surfactant interaction: Aggregation and dissolution of yellowish in N-dodecylpyridinum chloride, Fluid Phase Equilib. 239 (2) (2006) 166–171, https://doi.org/10.1016/j.fluid.2005.11.025.
[14] A.A. Rafati, S. Azizian, M. Chahardoli, Conductometric studies of interaction between anionic dyes and cetylpyridinium bromide in water–alcohol mixed solvents, J. Mol. Liq. 137 (1–3) (2008) 80–87, https://doi.org/10.1016/j.molliq.2007.03.013.
[15] S.M. Ghoreishi, M. Behpour, M. Shabani-Nooshabadi, Interaction of anionic azo dye and TTAB - cationic surfactant, J. Braz. Chem. Soc. 20 (3) (2009) 460–465, https://doi.org/10.1590/S0103-50532009000300008.
[16] B. Sohrabi, A. Bazyari, M. Hashemianzadeh, Effect of ethylene glycol on micellization and surface properties of Gemini surfactant solutions, Colloid Surf. A 364 (1–3) (2010) 87–93, https://doi.org/10.1016/j.colsurfa.2010.04.042.
[17] X.-H. Cheng, Y. Peng, C. Gao, Y. Yan, J.-B. Huang, Studying of 1-D assemblies in anionic azo dyes and cationic surfactants mixed systems, Colloid Surf. A: Physicochem. Eng. Aspects 422 (2013) 10–18, https://doi.org/10.1016/j.colsurfa.2012.12.062.
[18] B. Simončič, J. Špan, A study of dye-surfactant interactions. Part 1. Effect of chemical structure of acid dyes and surfactants on the complex formation, Dyes Pigm. 36 (1) (1998) 1–14, https://doi.org/10.1016/S0143-7208(97)00001-6.
[19] M.J. Minch, S.S. Shah, Spectroscopic studies of hydrophobic association. Merocyanine dyes in cationic and anionic micelles, J. Org. Chem. 44 (18) (1979) 3252–3255, https://doi.org/10.1021/jo01332a033.
[20] S.P. Moulik, S. Ghosh, A.R. Das, Interaction of acridine orange monohydrochloride dye with sodiumdodecylsulfate, (SDS) cetyltrimethylammoniumbromide (CTAB) and p-tert-octylphenoxypolyoxy ethanol (Triton X 100) surfactants, Colloid Polym. Sci. 257 (6) (1979) 645–655, https://doi.org/10.1007/BF01548834.
[21] M.F. Nazar, S.S. Shah, M.A. Khosa, Interaction of azo dye with cationic surfactant under different pH conditions, J. Surfact. Deterg. 13 (2010) 529–537, https://doi.org/10.1007/s11743-009-1177-8.
[22] E. Akpinar, G. Topcu, D. Reis, A.M.F. Neto, Effect of the anionic azo dye Sunset Yellow in lyotropic mixtures with uniaxial and biaxial nematic phases, J. Mol. Liq. 318 (2020), https://doi.org/10.1016/j.molliq.2020.114010 114010.
[23] E. Akpinar, N. Uygur, O. Demir-Ordu, D. Reis, A.M.F. Neto, Effect of the surfactant head-group size dependence of the dye-surfactant interactions on the lyotropic uniaxial to biaxial nematic phase transitions, J. Mol. Liq. 332 (2021), https://doi.org/10.1016/j.molliq.2021.115842 115842.
[24] A.A. Shahir, S. Javadian, B.B.M. Razavizadeh, H. Gharibi, Comprehensive study of tartrazine/cationic surfactant interaction, J. Phys. Chem. B 115 (49) (2011) 14435–14444, https://doi.org/10.1021/jp2051323.
[25] A. Ali, M. Alam, U. Farooq, S. Uzair, Effect of the nature of counterion on the micellar properties of cationic surfactants: a conductometric study, Phys. Chem. Liq. 56 (4) (2018) 528–543, https://doi.org/10.1080/00319104.2017.1358363.
[26] S. Streubel, F. Schulze-Zachau, E. Weißenborn, B. Braunschweig, Ion pairing and adsorption of azo dye/C16TAB surfactants at the air–water interface, J. Phys. Chem. C 121 (50) (2017) 27992–28000, https://doi.org/10.1021/acs.jpcc.7b08924.
[27] O.S. Esan, Temperature dependence on the molecular interaction of amaranth dye with cetyltrimethylammonium bromide in the premicelle region: A spectroscopy study, Chem. Sci. Eng. Res. 2 (3) (2020) 21–26, https://doi.org/10.36686/Ariviyal.CSER.2020.02.03.012.
[28] K.K. Karukstis, D.A. Savin, C.T. Loftus, N.D. D'Angelo, Spectroscopic studies of the interaction of methyl orange with cationic alkyltrimethylammonium

bromide surfactants, J. Colloid Interface Sci. 203 (1) (1998) 157–163, https://doi.org/10.1006/jcis.1998.5494.
[29] A.R. Petcu, E.A. Rogozea, C.A. Lazar, N.L. Olteanu, A. Meghea, M. Mihaly, Specific interactions within micelle microenvironment in different charged dye/surfactant systems, Arab. J. Chem. 9 (1) (2016) 9–17, https://doi.org/10.1016/j.arabjc.2015.09.009.
[30] S. Ghosh, S. Mondal, S. Das, R. Biswas, Spectroscopic investigation of interaction between crystal violet and various surfactants (cationic, anionic, nonionic and gemini) in aqueous solution, Fluid Phase Equilib. 332 (2012) 1–6, https://doi.org/10.1016/j.fluid.2012.06.019.
[31] M. Rashidi-Alavijeh, S. Javadian, H. Gharibi, M. Moradi, A.R. Tehrani-Bagha, A. A. Shahir, Intermolecular interactions between a dye and cationic surfactants: Effects of alkyl chain, head group, and counterion, Colloids Surf. A: Physicochem. Eng. Aspects 380 (1–3) (2011) 119–127, https://doi.org/10.1016/j.colsurfa.2011.02.011.
[32] M. Abe, T. Kasuya, K. Ogino, Thermodynamics of surfactant-dye complex formation in aqueous solutions. Sodium alkyl sulfates and azo oil dye systems, Colloid Polym. Sci. 266 (2) (1988) 156–163, https://doi.org/10.1007/BF01452813.
[33] Q. Ain, S. Khurshid, Z. Gul, J. Khatoon, M.R. Shah, I. Hamid, I.A.T. Khan, F. Aslam, Anionic azo dyes removal from water using aminefunctionalized cobalt–iron oxide nanoparticles: a comparative time-dependent study and structural optimization towards the removal mechanism, RSC Adv. 10 (2) (2020) 1021–1041, https://doi.org/10.1039/C9RA07686G.
[34] M. Abe, M. Ohsato, K. Ogino, Interaction between anionic surfactants and oil dye in the aqueous solutions. IV. The effect of alkyl chain length in surfactant molecule on the protonation equilibrium of azo dye, Colloid Polym. Sci. 262 (8) (1984) 657–661, https://doi.org/10.1007/BF01452458.
[35] H. Tajalli, A.G. Gilani, M.S. Zakerhamidi, M. Moghadam, Effects of surfactants on the molecular aggregation of rhodamine dyes in aqueous solutions, Spectrochim Acta A: Mol. Biomol. Spect. 72 (4) (2009) 697–702, https://doi.org/10.1016/j.saa.2008.09.033.
[36] F. Würthner, T.E. Kaiser, C.R. Saha-Möller, J-Aggregates: From serendipitous discovery to supramolecular engineering of functional dye materials, Angew. Chem. Int. Ed. 50 (15) (2011) 3376–3410, https://doi.org/10.1002/anie.201002307.
[37] L. Zhang, J.M. Cole, Dye aggregation in dye-sensitized solar cells, J. Mater. Chem. A 5 (37) (2017) 19541–19559, https://doi.org/10.1039/C7TA05632J.
[38] J.L. Bricks, Y.L. Slominskii, I.D. Panas, A.P. Demchenko, Fluorescent J-aggregates of cyanine dyes: basic research and applications review, Methods Appl. Fluoresc. 6 (1) (2018), https://doi.org/10.1088/2050-6120/aa8d0d 012001.
[39] M.E.D. Garcia, A. Sanz-Medel, Dye-surfactant interactions: a review, Talanta 33 (3) (1986) 255–264, https://doi.org/10.1016/0039-9140(86)80060-1.
[40] L. García-Río, P. Hervella, J.C. Mejuto, M. Parajó, Spectroscopic and kinetic investigation of the interaction between crystal violet and sodium dodecylsulfate, Chem. Phys. 335 (2–3) (2007) 164–176, https://doi.org/10.1016/j.chemphys.2007.04.006.
[41] J. Lydon, Chromonic review, J. Mater. Chem. 20 (45) (2010) 10071–10099, https://doi.org/10.1039/b926374h.
[42] V.V. Berejnov, V. Cabuil, R. Perzynski, Y.L. Raikher, S.N. Lysenko, V.N. Sdobnov, Lyotropic nematogenic system potassium laurate/1-decanol/water: method of synthesis and study of phase diagrams, Cryst. Rep. 45 (3) (2000) 493–500, https://doi.org/10.1134/1.171224.
[43] E. Akpinar, K. Otluoglu, M. Turkmen, C. Canioz, D. Reis, A.M.F. Neto, Effect of the presence of strong and weak electrolytes on the existence of uniaxial and biaxial nematic phases in lyotropic mixtures, Liq. Cryst. 43 (11) (2016) 1693–1708, https://doi.org/10.1080/02678292.2016.1194491.
[44] V.R. Horowitz, L.A. Janowitz, A.L. Modic, P.A. Heiney, P.J. Collings, Aggregation behavior and chromonic liquid crystal properties of an anionic monoazo dye, Phys. Rev. E 72 (2005), https://doi.org/10.1103/PhysRevE.72.041710 041710.
[45] H.-S. Park, S.-W. Kang, L. Tortora, Y. Nastishin, D. Finotello, S. Kumar, O.D. Lavrentovich, Self-assembly of lyotropic chromonic liquid crystal sunset yellow and effects of ionic additives, J. Phys. Chem. B 112 (51) (2008) 16307–16319, https://doi.org/10.1021/jp804767z.
[46] D.J. Edwards, J.W. Jones, O. Lozman, A.P. Ormerod, M. Sintyureva, G.J.T. Tiddy, Chromonic liquid crystal formation by edicol Sunset Yellow, J. Phys. Chem. B 112 (46) (2008) 14628–14636, https://doi.org/10.1021/jp802758m.
[47] D.N. Li, Y.X. Zhang, Z.H. Ren, L.L. Cai, J. Huang, B.B. Li, Q.H. Zhang, M.T. Yi, X.F. Quan, Y.X. Wang, B.R. Wang, Z.B. Qian, J.R. Wang, H. Tian, J. Yuan, N. Wang, Q.L. Long, X.M. Zhang, Molecular interaction for quasi-binary mixture of N-acyl amino sulfonate amphoteric surfactant from castor oil and stearyltrimethyl ammonium bromide, J. Mol. Liq. 339 (2021), https://doi.org/10.1016/j.molliq.2021.116813 116813.
[48] A. Chatterjee, S.P. Moulik, S.K. Sanyal, B.K. Mishra, P.M. Puri, Thermodynamics of micelle formation of ionic surfactants: A critical assessment for sodium dodecyl sulfate, cetyl pyridinium chloride and dioctyl sulfosuccinate (Na Salt) by microcalorimetric, conductometric, and tensiometric measurements, J. Phys. Chem. B 105 (51) (2001) 12823–12831, https://doi.org/10.1021/jp0123029.
[49] C. Das, D.K. Hazra, Micellization behaviour of lithium dodecyl sulphate in aqueous solutions using conductivity, density and adiabatic compressibility measurements, Ind. J. Chem. 44 (9) (2005) 1793–1799.
[50] K. Maiti, D. Mitra, S. Guha, S.P. Moulik, Salt effect on self-aggregation of sodium dodecylsulfate (SDS) and tetradecyltrimethylammonium bromide (TTAB): Physicochemical correlation and assessment in the light of hofmiester (lyotropic) effect, J. Mol. Liq. 146 (1–2) (2009) 44–51, https://doi.org/10.1016/j.molliq.2009.01.014.
[51] K.M. Sachin, S.A. Karpe, M. Singh, A. Bhattarai, Study on surface properties of sodiumdodecyl sulfate and dodecyltrimethylammonium bromide mixed surfactants and their interaction with dyes, Heliyon 5 (4) (2019), https://doi.org/10.1016/j.heliyon.2019.e01510 e01510.
[52] N.K. Chaudhary, A. Bhattarai, B. Guragain, A. Bhattarai, Conductivity, surface tension, and comparative antibacterial efficacy study of different brands of soaps of Nepal, J. Chem. 2020 (2020), https://doi.org/10.1155/2020/6989312 6989312.
[53] B. Everitt, The Cambridge Dictionary of Statistics, Cambridge University Press, Cambridge, UK New York, 1998, p. 67.
[54] J. Huang, Z.H. Ren, Micellization and interactions for ternary mixtures of amino sulfonate surfactant and nonionic octylphenol polyoxyethylene ethers in aqueous solution: 1 Blending with nonionic surfactants with smaller numbers of hydrophilic unit, J. Mol. Liq. 278 (2019) 53–60, https://doi.org/10.1016/j.molliq.2019.01.035.
[55] Z.H. Ren, J. Huang, Y.C. Zheng, L. Lai, L.L. Hu, Interaction and micellar behavior of binary mixture of amino sulfonate amphoteric surfactant with octadecyltrimethylammonium bromide in aqueous solutions of NaCl, J. Chem. Eng. Data 62 (6) (2017) 1782–1787, https://doi.org/10.1021/acs.jced.6b00968.
[56] Z.H. Ren, J. Huang, Y. Luo, Y.C. Zheng, P. Mei, W.C. Yu, L. Lai, Y.L. Chang, F.X. Lia, Effect of isopropanol on the micellization of binary mixtures containing amino sulfonate amphoteric surfactant in aqueous solution: Mixing with octadecyltrimethyl ammonium bromide, Colloids Surf. A 504 (2016) 131–138, https://doi.org/10.1016/j.colsurfa.2016.05.063.
[57] R.J. Williams, J.N. Phillips, K.J. Mysels, The critical micelle concentration of sodium lauryl sulphate at 25°C, Trans. Faraday Soc. 51 (1955) 728–737, https://doi.org/10.1039/TF9555100728.
[58] M. Pérez-Rodríguez, G. Prieto, C. Rega, L.M. Varela, F. Sarmiento, V. Mosquera, A comparative study of the determination of the critical micelle concentration by conductivity and dielectric constant measurements, Langmuir 14 (16) (1998) 4422–4426, https://doi.org/10.1021/la980296a.
[59] P. Carpena, J. Aguiar, P. Bernaola-Galvan, C.C. Ruiz, Problems associated with the treatment of conductivity-concentration data in surfactant solutions: Simulations and experiments, Langmuir 18 (16) (2002) 6054–6058, https://doi.org/10.1021/la025770y.
[60] P.A. Koya, T.A. Wagay, K. Ismail, Conductometric studies on micellization of cationic surfactants in the presence of glycine, J. Sol. Chem. 44 (2015) 100–111, https://doi.org/10.1007/s10953-014-0284-y.
[61] P. Zheng, D. Cai, K. Qiao, J. Zhao, W. Shen, Temperature dependence of micellization behavior of N', N'-didodecyl-N, N, N', N'-tetramethylhexane-1,6-diammonim dibromide and 1-dodecyl-3-methylimidazolium bromide in aqueous solutions, J. Mol. Liq. 308 (2020), https://doi.org/10.1016/j.molliq.2020.112999 112999.
[62] S.P. Musale, P.S. Babalsure, D.D. Pawar, Volumetric properties, viscosity coefficients and aggregation behaviour of DBU-acetate protic ionic liquid in molecular solvents, J. Mol. Liq. 319 (2020), https://doi.org/10.1016/j.molliq.2020.114197 114197.
[63] J. Aguiar, P. Carpena, J.A. Molina-Bolívar, C.C. Ruiz, On the determination of the critical micelle concentration by the pyrene 1:3 ratio method, J. Colloid Interface Sci. 258 (1) (2003) 116–122, https://doi.org/10.1016/S0021-9797(02)00082-6.
[64] G. Sugihara, T.-Y. Nakano, S.B. Sulthana, A.K. Rakshit, Enthalpy-entropy compensation rule and compensation temperature observed in micelle formation of different surfactants in water. What is the so-called compensation temperature?, J Oleo Sci. 50 (1) (2001) 29–39, https://doi.org/10.5650/jos.50.29.
[65] M.J. Rosen, Surfactants and Interfacial Phenomena, second ed., Wiley, New York, 1989.
[66] A.D. Fenta, Surface and thermodynamic studies of micellization of surfactants in binary mixtures of 1,2-ethanediol and 1,2,3-propanetriol with water, Int. J. Phys. Sci. 10 (8) (2015) 276–288, https://doi.org/10.5897/IJPS2015.4288, 4962B2A52349.
[67] S. Ghosh, S.P. Moulik, Interfacial and micellization behaviors of binary and ternary mixtures of amphiphiles (Tween-20, Brij-35, and sodium dodecyl sulfate) in aqueous medium, J. Colloid Interface Sci. 208 (2) (1998) 357–366, https://doi.org/10.1006/jcis.1998.5752.
[68] J. Oremusova, Z. Vitkova, A. Vitko, M. Tarnik, E. Miklovicova, O. Ivankova, J. Murgas, D. Krchnak, Effect of molecular composition of head group and temperature on micellar properties of ionic surfactants with C12 alkyl chain, Molecules 24 (3) (2014), https://doi.org/10.3390/molecules24030651 651.
[69] S. Mahbub, M. Rahman, S. Rana, M.A. Rub, M.A. Hoque, M.A. Khan, A.M. Asiri, Aggregation behavior of sodium dodecyl sulfate and cetyltrimethylammonium bromide mixtures in aqueous/chitosan solution at various temperatures: An experimental and theoretical approach, J. Surf. Deterg. 22 (1) (2019) 137–152, https://doi.org/10.1002/jsde.12202.
[70] K.M. Kale, R. Zana, Effect of the nature of the counterion on the volume change upon micellization of ionic detergents in aqueous solutions, J. Colloid Interface Sci. 61 (2) (1977) 312–322, https://doi.org/10.1016/0021-9797(77)90394-0.
[71] S.K. Mehta, K.K. Bhasin, R. Chauhan, S. Dham, Effect of temperature on critical micelle concentration and thermodynamic behavior of dodecyldimethylethylammonium bromide and dodecyltrimethylammonium chloride in aqueous media, Colloid Surf. A 255 (1–3) (2005) 153–157, https://doi.org/10.1016/j.colsurfa.2004.12.038.
[72] E. Fisicaro, M. Biemmi, C. Compari, E. Duce, M. Peroni, Thermodynamics of aqueous solutions of dodecyldimethylethylammonium bromide, J. Colloid Interface Sci. 305 (2) (2007) 301–307, https://doi.org/10.1016/j.jcis.2006.09.063.

[73] E. Junquera, E. Aicart, Mixed micellization of dodecylethyldimethylammonium bromide and dodecyltrimethylammonium bromide in aqueous solution, Langmuir 18 (24) (2002) 9250–9258, https://doi.org/10.1021/la026121p.
[74] B.L. Bales, R. Zana, Characterization of micelles of quaternary ammonium surfactants as reaction media I: Dodecyltrimethylammonium bromide and chloride, J. Phys. Chem. B 106 (8) (2002) 1926–1939, https://doi.org/10.1021/jp013813y.
[75] A. Malliaris, J. Le Moigne, J. Sturm, R. Zana, Temperature dependence of the micelle aggregation number and rate of intramicellar excimer formation in aqueous surfactant solutions, J. Phys. Chem. 89 (12) (1985) 2709–2713, https://doi.org/10.1021/j100258a054.
[76] B. Šarac, M. Bešter-Rogač, Temperature and salt-induced micellization of dodecyltrimethylammonium chloride in aqueous solution: A thermodynamic study, J. Colloid Interface Sci. 338 (1) (2009) 216–221, https://doi.org/10.1016/j.jcis.2009.06.027.
[77] J. Bach, M.J. Blandamer, K. Bijma, J.P.F.N. Engberts, P.A. Kooreman, A. Kacperska, K.C. Rao, M.C.S. Subha, Titration calorimetric and spectrophotometric studies of micelle formation by alkyltrimethylammonium bromide in aqueous solution, J. Chem. Soc. Fraday Trans. 91 (1995) 1229–1235, https://doi.org/10.1039/FT9959101229.
[78] R. Zieliński, S. Ikeda, H. Nomura, S. Kato, Effect of temperature on micelle formation in aqueous solutions of alkyltrimethylammonium bromides, J. Colloid Interface Sci. 129 (1) (1989) 175–184, https://doi.org/10.1016/0021-9797(89)90428-1.
[79] J.L. López-Fontán, M.J. Suárez, V. Mosquera, F. Sarmiento, Mixed micelles of n-alkyltrimethylammonium bromides: influence of alkyl chain length, Phys. Chem. Chem. Phys. 1 (15) (1999) 3583–3587, https://doi.org/10.1039/A903532J.
[80] A. Ghasemi, A. Bagheri, Effects of alkyl chain length on synergetic interaction and micelle formation between a homologous series of n-alkyltrimethylammonium bromides and amphiphilic drug propranolol hydrochloride, J. Mol. Liq. 298 (2020), https://doi.org/10.1016/j.molliq.2019.111948 111948.
[81] R. Jaber, M.J. Wasbrough, J.A. Holdaway, K.J. Edler, Interactions between quaternary ammonium surfactants and polyethylenimine at high pH in film forming systems, J. Colloid Interface Sci. 449 (2015) 286–296, https://doi.org/10.1016/j.jcis.2015.01.034.
[82] K. Kalyanasundram, Photochemistry im Microheterogeneous Systems, Academic Press, New York, 1987.
[83] C.C. Ruiz, A photophysical study of micellization of cetyltrimethylammonium bromide in urea-water binary mixtures, Mol. Phys. 86 (3) (1995) 535–546, https://doi.org/10.1080/00268979509413628.
[84] V. Peyre, S. Bouguerra, F. Testard, Micellization of dodecyltrimethylammonium bromide in water-dimethylsulfoxide mixtures: A multi-length scale approach in a model system, J. Colloid Interface Sci. 389 (1) (2013) 164–174, https://doi.org/10.1016/j.jcis.2012.08.014.
[85] S. Chauhan, M. Kaur, K. Kumar, M.S. Chauhan, Study of the effect of electrolyte and temperature on the critical micelle concentration of dodecyltrimethylammonium bromide in aqueous medium, J. Chem. Thermodynamics 78 (2014) 175–181, https://doi.org/10.1016/j.jct.2014.07.003.
[86] J. Aguiar, J.A. Molina-Bolivar, J.M. Peula-Garcia, C.C. Ruiz, Thermodynamics and micellar properties of tetradecyltrimethylammonium bromide in formamide–water mixtures, J. Colloid Interface Sci. 255 (2) (2002) 382–390, https://doi.org/10.1006/jcis.2002.8678.
[87] M.T. Muhammad, M.N. Khan, Oppositely charged dye surfactant interactions: Extent and selectivity of ion pair formation, J. Mol. Liq. 266 (2018) 591–596, https://doi.org/10.1016/j.molliq.2018.06.108.
[88] A. Navarro, F. Sanz, Dye aggregation in solution: study of C.I. direct red I, Dyes Pigm. 40 (2–3) (1999) 131–139, https://doi.org/10.1016/S0143-7208(98)00048-5.
[89] G.B. Behera, P.K. Behera, B.K. Mishra, Cyanine dyes: self aggregation and behaviour in surfactants a review, J. Surf. Sci. Technol. 23 (1–2) (2007) 1–31, https://doi.org/10.18311/jsst/2007/1958.
[90] Y. Wang, Z. Zhang, Y. Xiao, N. Li, Spectrophotometric determination of Sunset Yellow in beverage after preconcentration by the cloud point extraction method, Anal. Methods 6 (22) (2014) 8901–8905, https://doi.org/10.1039/C4AY01537A.
[91] G.E. do Nascimento, V.O.M. Cavalcanti, R.M.R. Santana, D.C.S. Sales, J.M. Rodríguez-Díaz, D.C. Napoleão, M.M.M.B. Duarte, Degradation of a Sunset Yellow and Tartrazine dye mixture: Optimization using statistical design and empirical mathematical modeling, Water Air Soil Pollut. 231 (2020), https://doi.org/10.1007/s11270-020-04547-5 254.
[92] P. Oancea, V. Meltzer, Photo-Fenton process for the degradation of tartrazine (E102) in aqueous medium, J. Taiwan Inst. Chem. Eng. 44 (6) (2013) 990–994, https://doi.org/10.1016/j.jtice.2013.03.014.
[93] M.M. Ghoneim, H.S. El-Desoky, N.M. Zidan, Electro-Fenton oxidation of sunset yellow FCF azo-dye in aqueous solutions, Desalination 274 (1–3) (2011) 22–30, https://doi.org/10.1016/j.desal.2011.01.062.
[94] A. Fernández-Pérez, G. Marbán, Visible light spectroscopic analysis of methylene blue in water; What comes after dimer?, ACS Omega 5 (46) (2020) 29801–29815, https://doiorg/10.1021/acsomega.0c03830.